Nanotechnology

DOI: 10.1002/anie.201205929

High-Yield Synthesis of Silver Nanoclusters Protected by DNA Monomers and DFT Prediction of their Photoluminescence Properties**

Xuan Yang, Linfeng Gan, Lei Han, Erkang Wang, and Jin Wang**

Silver nanoclusters have attracted much research interest because of their unique size-dependent optical, electronic, magnetic, and catalytic properties that bridge the gap between small molecules (e.g., organometallic compounds) and bulk crystals (diameter typically >2 nm).[1–8] As the size of silver nanoparticles decreases to the Fermi wavelength of an electron, discrete energy levels begin to form, allowing the interaction with light through electronic transitions between different energy levels, resulting in strong photoluminescence. Such silver nanoclusters are considered suitable labels for the study of biological systems, and different ligands are utilized for the synthesis of fluorescent silver nanoclusters through various approaches.[1–8]

Continued research efforts have been directed toward possible applications of DNA since its discovery.[9] Today, DNA oligonucleotides are utilized, among other things, as scaffolds for silver nanoclusters, and many research groups are dedicated to the study of DNA-protected silver nanoclusters.[1,2,10–13] Both single-stranded DNA and DNA duplexes are utilized as the scaffolds for fluorescent silver nanoclusters,[10–13] and even nanoclusters stabilized by triplex DNA strands can be synthesized.[14] Despite the existence of various silver nanoclusters stabilized by different DNA strands, programmed synthesis of DNA-stabilized silver nanoclusters with photoluminescence properties has not been achieved. Because of the complexity of DNA strands, there is still no satisfactory synthetic approach to fluorescent silver nanoclusters with DNA as the scaffold.[1,10–13]

In this study, we developed a high-yield synthesis of silver nanoclusters using DNA monomers as the scaffolds for the first time. Most of the silver nanoclusters are formed with nine silver atoms, and only the silver nanoclusters protected by deoxycytidine monomers (dC) show fluorescence emissions. Herein, we explain the mechanism of the formation of DNA-protected silver nanoclusters and the reason why cytosine-rich DNA strands are good scaffolds for fluorescent silver nanoclusters. We carried out density-functional computations to predict the fluorescence of dC-protected silver nanoclusters, and the results are in very good agreement with the experiments. Therefore, we not only synthesized silver nanoclusters protected by DNA monomers for the first time, but also predicted their photoluminescence properties. Our results provide basic guidelines for further experimental and theoretical studies on DNA-protected fluorescent silver nanoclusters and may ultimately contribute to the programmed synthesis of DNA-stabilized silver nanoclusters with photoluminescence properties. The fine control of the properties of DNA-stabilized silver nanoclusters suggests many possible uses, ranging from biology to nanoscience.

Transmission electron microscopy (TEM) was used to directly observe the size distributions of the silver nanoclusters protected by DNA monomers and thus characterize their nanostructure. The diameters of most silver nanoclusters stabilized by deoxyadenosine monomers (dA) ranged from 0.5 to 2.0 nm, which is consistent with the definition of nanoclusters (<2 nm; Figure 1 A,B). There might have been some smaller nanoclusters present, but because of the low resolution of the transmission electron microscope, these nanoclusters were not observed. These nanoparticles with diameters ranging from 0.5 to 2.0 nm might be aggregations of small nanoclusters. Energy-dispersive spectroscopy (EDS) showed that such silver nanoclusters with dA as scaffolds mainly consisted of elemental silver (see the Suppporting Information, Figure S3). To estimate the protective ability of DNA for silver nanoclusters, the other three deoxynucleoside monomers were also used in the synthesis of silver nanoclusters. The diameters of nanoparticles protected by these three monomers were mostly in the range from 0.5 to 2.5 nm (Figure 1). The EDS results showed that these nanoclusters also consisted of elemental silver (Supporting Information, Figures S3 and S4). The results of TEM and EDS indicated that deoxythymidine monomers (dT), dC, and deoxyguanosine monomers (dG) could also be used as scaffolds for the synthesis of silver nanoclusters. Therefore, we suspected that

[*] X. Yang,[+] L. Gan,[+] L. Han, Prof. E. Wang, Prof. J. Wang
State Key Laboratory of Electroanalytical Chemistry
Changchun Institute of Applied Chemistry
Changchun, Jilin, 130022 (P.R. China)
and
Chinese Academy of Sciences, University of Chinese Academy of Sciences, Beijing, 100039 (P.R. China)
E-mail: ekwang@ciac.jl.cn
jin.wang.1@stonybrook.edu
Prof. J. Wang
College of Physics, Jilin University
Changchun, Jilin, 130012 (P.R. China)
and
Department of Chemistry and Physics
State University of New York at Stony Brook
Stony Brook, NY 11794-3400 (USA)

[+] These authors contributed equally to this work.

[**] This work was supported by the National Natural Science Foundation of China (grant numbers 21190040 and 11174105, and 973 Projects 2009CB930100 and 2010CB933600) and the National Science Foundation.

Supporting information for this article is available on the WWW under http://dx.doi.org/10.1002/anie.201205929.

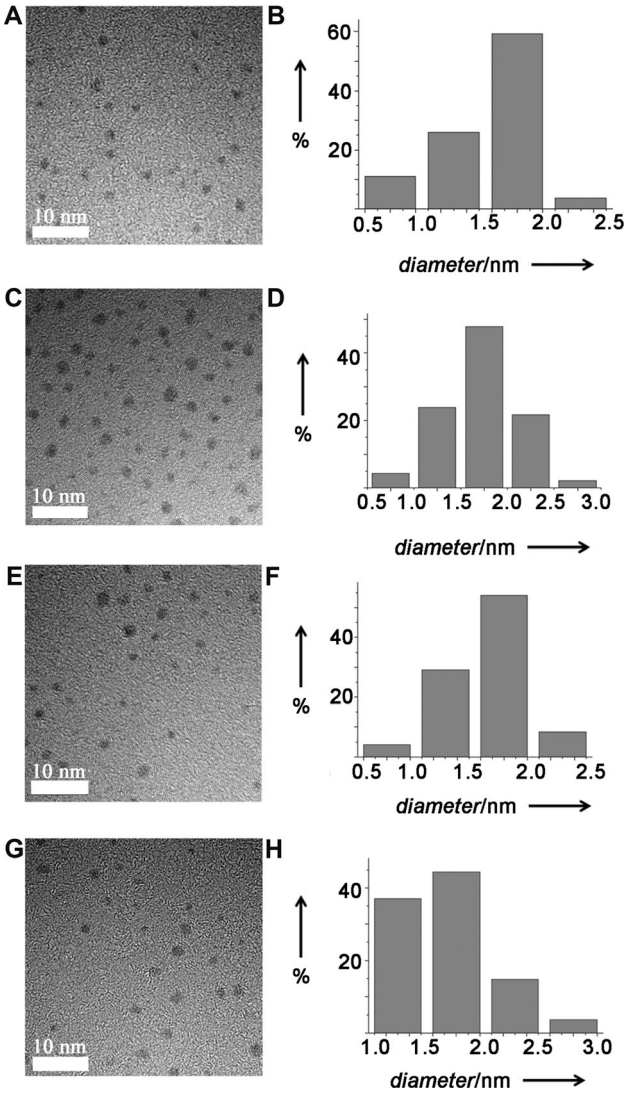

Figure 1. Typical TEM images and particle size distributions of silver nanoclusters protected by different scaffolds: dA (A, B), dT (C, D), dC (E, F), and dG (G, H).

the protective abilities of the monomers might originate from the affinity of silver to the pyrimidine or purine base,[1,2,10,11] which could be one of the reasons why DNA strands are good scaffolds for silver nanoclusters. The results of X-ray diffraction (XRD) and X-ray photoelectron spectroscopy (XPS) of these silver nanoclusters are shown in Figure S5 in the Supporting Information.

In order to determine the actual structures of the silver nanoclusters and the number of silver atoms that are aggregated in these nanoclusters, matrix-assisted laser desorption/ionization time-of-flight/time-of-flight mass spectrometry (MALDI-TOF/TOF-MS) was employed. The MALDI-TOF/TOF mass spectrum of dA-protected silver nanoclusters showed that the nanoclusters contained a small number of silver atoms, such as Ag_7, Ag_9, Ag_{11}, Ag_{13}, Ag_{15}, Ag_{17}, Ag_{19}, and Ag_{21}, and that most of the nanoclusters contained Ag_9 (Figure 2A). Nanoclusters with even numbers of silver atoms were not observed. The theoretically calculated isotopic pattern for Ag_9 of dA-protected silver nanoclusters was in very good agreement with the experimental pattern (Supporting Information, Figure S6). The MALDI-TOF/TOF mass spectra showed similar patterns for dT- and dA-protected silver nanoclusters. Some silver nanoclusters were formed with odd numbers of silver atoms, such as Ag_7, Ag_9, Ag_{11}, Ag_{13}, Ag_{15}, Ag_{17}, Ag_{19}, and Ag_{21}, however, nanoclusters with an even number of silver atoms were not formed. The intensity of the Ag_9 signal was also the highest among the signals of dT-protected silver nanoclusters (Figure 2B), and thus, the nanoclusters consisted mainly of Ag_9. Furthermore, the simulated isotopic patterns for the Ag_9 in dT-protected silver nanoclusters were consistent with the experimental patterns (Supporting Information, Figure S7). Figure 2C shows the MALDI-TOF/TOF mass spectra of silver nanoclusters protected with dC. Only the signals for Ag_9 were observed; the signals of clusters with a different number of silver atoms were small enough that they could be ingnored. The experimentally obtained and theoretically calculated isotopic patterns for Ag_9 in dC-protected silver nanoclusters are shown in Figure S8 in the Supporting Information. Figure 2D shows the MALDI-TOF/TOF mass spectrum of dG-protected silver nanoclusters, in which only the signal for Ag_7 can be observed. The MALDI-TOF/TOF mass spectra of these silver nanoclusters only contained signals of silver atoms; signals of DNA-protected nanoclusters were not present. These MS results were similar to those of poly-(methacrylic acid)-protected silver nanoclusters.[8] We assumed that the bond between the DNA monomers and silver atoms is not strong, and can thus be easily cleaved. This might be one of the reasons why silver nanoclusters with DNA as scaffold are not stable enough.

To investigate the optical properties of silver nanoclusters that are protected by DNA monomers, the nanoclusters were dissolved in chloroform for characterization by fluorescence and UV-visible absorption spectroscopy. Only dC-protected silver nanoclusters showed a strong fluorescent excitation at 519 nm and fluorescent emission at 591 nm, while the nanoclusters protected by dA, dT, and dG showed no fluorescence properties at all (Figure 3A). We believe that this property makes cytosine-rich DNA a good scaffold for fluorescent silver nanoclusters. The photoluminescence spectra confirmed that the fluorescence of the solution of dC-protected silver nanoclusters originated from the nanoclusters, and not from chloroform (Supporting Information, Figure S9). Figure 3B shows the UV-visible absorption spectra of the silver nanoclusters. Despite the similar structures of these four protective agents and the silver nanoclusters, there were some differences in the absorption spectra. The absorption peaks of dA-, dT-, dC-, and dG-protected silver nanoclusters were at 437, 442, 447, and 415 nm, respectively. The differences of the photoluminescence spectra and UV-visible absorption spectra showed that similar silver nanoclusters can have different optical properties.

As the bond between the monomers and silver atoms was very weak, Fourier-transform infrared spectroscopy (FTIR) was utilized to verify whether the monomers were attached to the surface of the silver nanoclusters and acted as protective agents. The four monomers displayed similar FTIR spectra

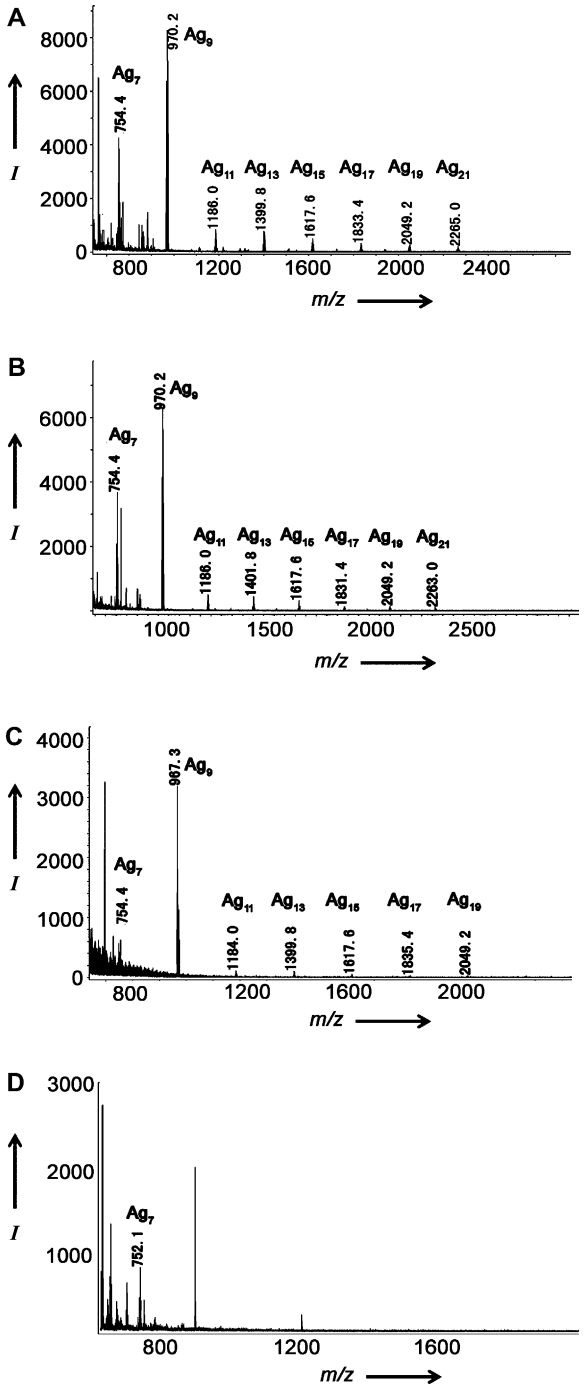

Figure 2. MALDI-TOF/TOF mass spectra of silver nanoclusters protected by different scaffolds: dA (A), dT (B), dC (C), and dG (D).

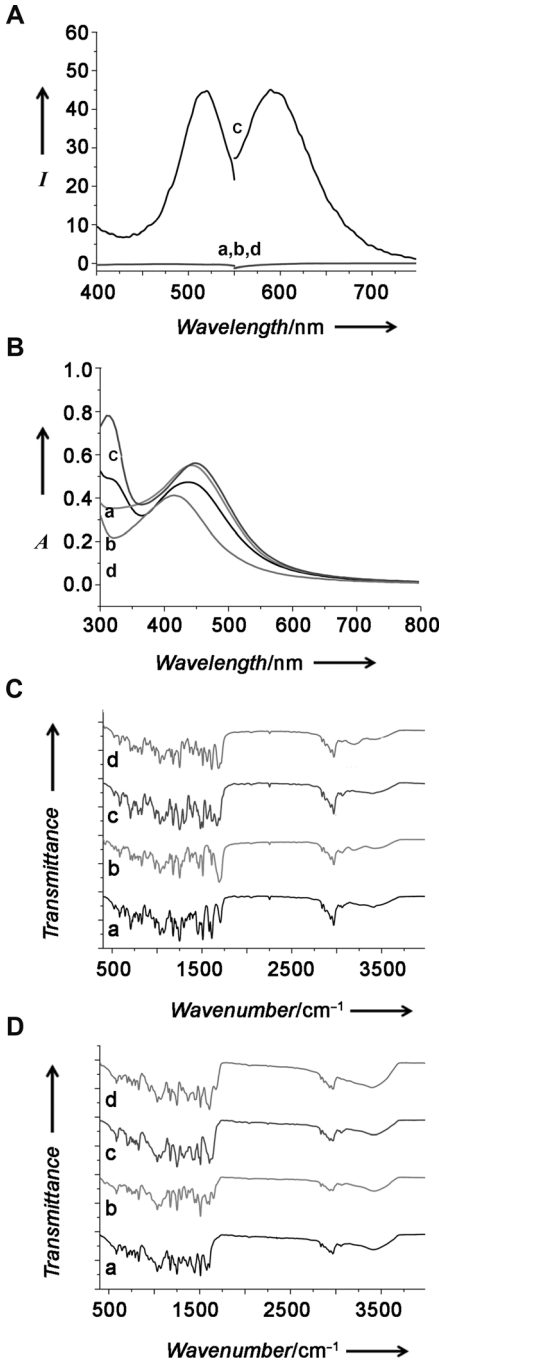

Figure 3. A) Photoluminescence spectra and B) UV-visible absorption spectra of silver nanoclusters protected by different scaffolds: dA (a), dT (b), dC (c), and dG (d) (in chloroform). FTIR spetra of C) DNA monomers: dA (a), dT (b), dC (c), and dG (d), and D) silver nanoclusters protected by different scaffolds: dA (a), dT (b), dC (c), and dG (d).

(Figure 3C), a result that is consistent with their analogous chemical structures (Supporting Information, Figure S2). The absorption band at about 2255 cm^{-1} apparently belongs to a C–N bonds, and the absorption band at about 2968 cm^{-1} belongs to C–H bonds. The two broad bands at about 3196 cm^{-1} and 3417 cm^{-1} could both be assigned to the stretching modes of N–H bonds. The FTIR spectra of the silver nanoclusters protected by dA, dT, dC, and dG (Figure 3D) showed similar bands at the same wavenumbers, which is again consistent with the similar chemical structures of the monomers. The absorption band at about 2968 cm^{-1} apparently belongs to C–H bonds, and an absorption band at about 3401 cm^{-1} belongs to N–H bonds, thus demonstrating that the monomers are linked to the silver atoms. A comparison of Figure 3C with 3D shows that there were very few differences between the free monomers and the monomers that protect the silver nanoclusters.

We carried out density-functional computations to explain the photoluminescence properties of dC-protected silver nanoclusters, and to assist the structural characterization and interpretation for this system.[15] After the random search of nearly 100 optimized random ground-state geometries, we found the geometry in which the Ag_9 cluster is attached to the amide group of benzoyl-protected cytosine (in dC) to be the lowest-energy configuration for the dC–Ag_9 complex. The structure of the lowest-energy configuration, which we called geometry 1A, is shown in Figure 4A. In order to interpret the emission spectra, we optimized the geometries of the excited states of Ag_9, dC, and the dC–Ag_9 complex by time-dependent density-functional theory (TDDFT). In our theoretical results, the dC–Ag_9 complex with an optimized structure based on geometry 1A showed an emission at 590 nm, which was consistent with our experimental results, and the structure was thus considered the optimal excited-state geometry of the dC–Ag_9 complex, which we called geometry 1B (Figure 4B). The distance between Ag34 of the Ag_9 cluster and O14 of the amide group of benzoyl-protected cytosine (in dC) was 2.63 Å, which is similar to the distance in hydrogen bonds. This might be the reason why in the FTIR spectra, the DNA-protected silver nanoclusters showed bands with similar shapes and at the same wavenumbers as the free DNA monomers, while in MALDI-TOF/TOF mass spectra no signal could be observed for the dC–Ag_9 complex. In our study, a strong calculated emission band at 590 nm corresponded to the 15th excited state of the dC–Ag_9 complex, which was consistent with the experimental emission band at 591 nm (Figure 4D). The excitations alpha HOMO−1-(141 A)→alpha LUMO + 1(144 A) (44%), alpha HOMO-(142 A)→alpha LUMO + 5(149 A) (6%), and beta HOMO-(141B)→beta LUMO + 2(144B) mainly contributed to the excited state (Figure 4C). The electron-density plots of these frontier molecular orbitals along with the highest-occupied and lowest-occupied molecular orbitals (HOMO and LUMO, respectively) are shown in Figure 4C. The LUMO orbitals were mostly composed of molecular orbitals of the entire Ag_9 cluster and the amide group of the benzoyl-protected cytosine (in dC). The simulation results indicated that the fluorescence emission band at 590 nm originated from both the Ag_9 cluster and the amide group.

The weak attractive interaction between Ag_9 and the dC monomer was studied by reduced-density gradient (RDG) analysis, reported by Yang and co-workers,[16] where RDG was defined as $RDG(\mathbf{r}) = |\nabla\rho(\mathbf{r})|/\rho^{4/3}(\mathbf{r})$ with ρ = electron density of the whole system. Yang and co-workers used Ω to identify the interaction type, $\Omega = \mathrm{sign}(\lambda_2)\rho$, in which $\mathrm{sign}(\lambda_2)$ is the sign of the second largest eigenvalue of the Hessian matrix of the electron density. The functions, such as RDG and Ω, were calculated with Multiwfn software.[17] The gradient isosurface was plotted with VMD (Figure 5A).[18]

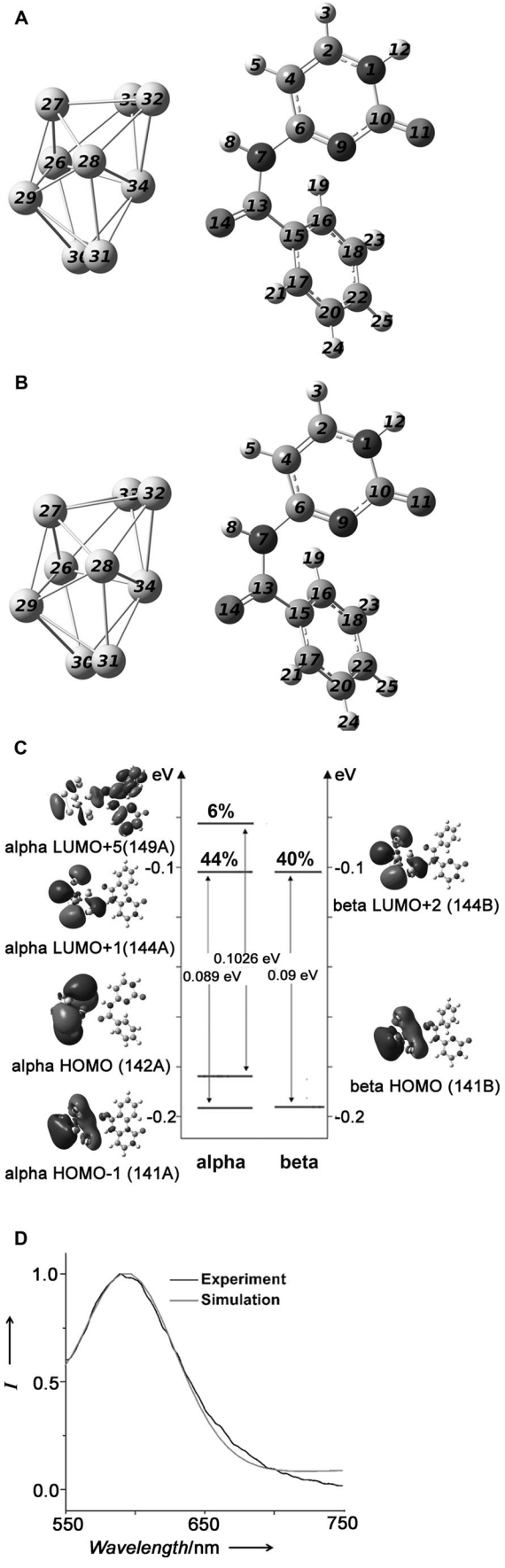

Figure 4. Optimal ground-state (A) and excited-state (B) geometries of the dC–Ag_9 complex. For clarity, only a benzoyl-protected cytosine base in proximity to the Ag_9 cluster is shown. C) Molecular orbitals and electronic contributions of the relevant excited states, and D) fluorescence spectra (black: experiment; gray: simulation) of the dC–Ag_9 complex.

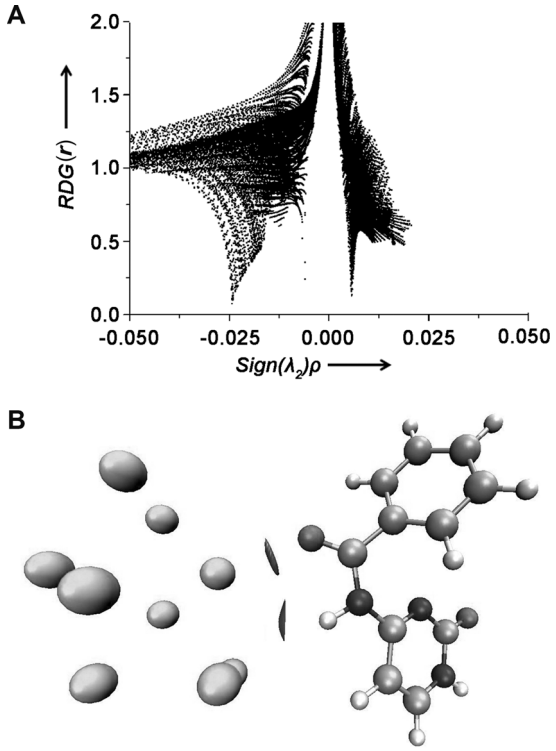

Figure 5. A) Reduced-density gradient (RDG(**r**)) plotted versus electron density (ρ) multiplied by sign(λ_2), B) gradient isosurface of interactions between Ag_9 and dC.

According to these calculations, Ω of the dC–Ag_9 complex was nearly −0.025 au, which maps to an interaction between a hydrogen bond and a van der Waals interaction. The interaction in the complex is strong enough to stabilize the complex. As anticipated, the gradient isosurface of the interface of the dC–Ag_9 complex showed a weak attractive interaction between Ag34 and O14 (Figure 5B). The characteristic steric attraction appears to be quite strong, which we believe is the reason for the unique quality of the dC–Ag_9 complex.

In summary, we have synthesized several silver nanoclusters with four different DNA monomers as scaffolds, which, to the best of our knowledge, has previously not been attempted. We have explored the formation mechanisms of DNA-protected silver nanoclusters and the roles of the four bases in the synthesis of silver nanoclusters with DNA scaffolds. Most of the nanoclusters are formed with nine silver atoms and only dC-protected silver nanoclusters show a strong fluorescence emission. These results provide basic evidence of the benefit of using cytosine-rich DNA strands for the synthesis of fluorescent silver nanoclusters.[12,13] At last, we carried out density-functional computations to calculate the fluorescence properties of silver nanoclusters with dC as scaffolds, and the results are in very good agreement with the experimental studies. The findings suggest that the fluorescence property of silver nanoclusters originates from both silver atoms and scaffolds. Therefore, the results provide basic guidelines for further experimental and theoretical studies on DNA-stabilized fluorescent silver nanoclusters and other scaffold-protected silver nanoclusters. Our study may ultimately contribute to achieving programmed synthesis of DNA-stabilized silver nanoclusters with photoluminescence properties. And we believe that the programmed synthesis of DNA-stabilized silver nanoclusters may have many further uses, ranging from biology to nanoscience.

Received: July 25, 2012
Published online: January 9, 2013

Keywords: cluster compounds · density functional calculations · DNA · fluorescence · silver

[1] T. Vosch, Y. Antoku, J. C. Hsiang, C. I. Richards, J. I. Gonzalez, R. M. Dickson, *Proc. Natl. Acad. Sci. USA* **2007**, *104*, 12616–12621.
[2] J. Zheng, R. M. Dickson, *J. Am. Chem. Soc.* **2002**, *124*, 13982–13983.
[3] Z. K. Wu, E. Lanni, W. Q. Chen, M. E. Bier, D. Ly, R. C. Jin, *J. Am. Chem. Soc.* **2009**, *131*, 16672–16673.
[4] O. M. Bakr, V. Amendola, C. M. Aikens, W. Wenseleers, R. Li, L. Dal Negro, G. C. Schatz, F. Stellacci, *Angew. Chem.* **2009**, *121*, 6035–6040; *Angew. Chem. Int. Ed.* **2009**, *48*, 5921–5926.
[5] J. G. Zhang, S. Q. Xu, E. Kumacheva, *Adv. Mater.* **2005**, *17*, 2336–2340.
[6] Z. Shen, H. W. Duan, H. Frey, *Adv. Mater.* **2007**, *19*, 349–352.
[7] L. Shang, S. J. Dong, *Chem. Commun.* **2008**, 1088–1090.
[8] I. Díez, M. Pusa, S. Kulmala, H. Jiang, A. Walther, A. S. Goldmann, A. H. E. Muller, O. Ikkala, R. H. A. Ras, *Angew. Chem.* **2009**, *121*, 2156–2159; *Angew. Chem. Int. Ed.* **2009**, *48*, 2122–2125.
[9] K. Sefah, G. D. Shang, X. L. Xiong, M. B. O'Donoghue, W. H. Tan, *Nat. Protoc.* **2010**, *5*, 1169–1185.
[10] W. W. Guo, J. P. Yuan, Q. Z. Dong, E. K. Wang, *J. Am. Chem. Soc.* **2010**, *132*, 932–934.
[11] C. I. Richards, S. Choi, J. C. Hsiang, Y. Antoku, T. Vosch, A. Bongiorno, Y. L. Tzeng, R. M. Dickson, *J. Am. Chem. Soc.* **2008**, *130*, 5038–5039.
[12] E. G. Gwinn, P. O'Neill, A. J. Guerrero, D. Bouwmeester, D. K. Fygenson, *Adv. Mater.* **2008**, *20*, 279–283.
[13] V. Soto-Verdugo, H. Metiu, E. Gwinn, *J. Chem. Phys.* **2010**, *132*, 195102.
[14] L. Y. Feng, Z. Z. Huang, J. S. Ren, X. G. Qu, *Nucl. Acids Res.* **2013**, DOI: 10.1093/nar/gks387.
[15] Z. X. Luo, G. U. Gamboa, J. C. Smith, A. C. Reber, J. U. Reveles, S. N. Khanna, A. W. Castleman, Jr., *J. Am. Chem. Soc.* **2012**, *134*, 18973–18978.
[16] E. R. Johnson, S. Keinan, P. Mori-Sanchez, J. Contreras-Garcia, A. J. Cohen, W. T. Yang, *J. Am. Chem. Soc.* **2010**, *132*, 6498–6506.
[17] T. Lu, F. W. Chen, *J. Comput. Chem.* **2012**, *33*, 580–592.
[18] W. Humphrey, A. Dalke, K. Schulten, *J. Mol. Graph. Model.* **1996**, *14*, 33–38.

